

Drivers of plant nutrient acquisition and allocation strategies and their influence  
on plant responses to environmental change

by

Evan A. Perkowski, B.S.

A Dissertation

In

Biological Sciences

Submitted to the Graduate Faculty  
of Texas Tech University in  
Partial Fulfillment of  
the Requirements for  
the Degree of

Doctor of Philosophy

Approved

Dr. Nicholas G. Smith  
Chair of Committee

Dr. Aimée T. Classen

Dr. Natasja van Gestel

Dr. Lindsey C. Slaughter

Dr. Dylan W. Schwilk

Dr. Mark Sheridan  
Dean of the Graduate School

May 2023

Copyright 2023, Evan A. Perkowski

## Acknowledgements

Placeholder for text

## Table of Contents

<b>Acknowledgements</b> . . . . .	ii
<b>Abstract</b> . . . . .	iv
<b>List of Tables</b> . . . . .	v
<b>List of Figures</b> . . . . .	vi
<b>1. Introduction</b> . . . . .	1
<b>2. Structural carbon costs to acquire nitrogen are determined by nitrogen and light availability in two species with different nitrogen acquisition strategies</b> . . . . .	2
2.1 Introduction . . . . .	2
2.2 Methods . . . . .	6
2.2.1 <i>Experiment setup</i> . . . . .	6
2.2.2 <i>Plant measurements and calculations</i> . . . . .	7
2.2.3 <i>Statistical analyses</i> . . . . .	8
2.3 Results . . . . .	10
2.3.1 <i>Carbon costs to acquire nitrogen</i> . . . . .	10
2.3.2 <i>Whole plant nitrogen biomass</i> . . . . .	13
2.3.3 <i>Root carbon biomass</i> . . . . .	15
2.3.4 <i>Root nodule biomass</i> . . . . .	17
2.4 Discussion . . . . .	21
<b>3. Soil nitrogen availability modifies leaf nitrogen economies in mature temperate deciduous forests: a direct test of photosynthetic least-cost theory</b> . . . . .	28
3.1 Introduction . . . . .	28
3.2 Methods . . . . .	29
3.3 Results . . . . .	29
<b>4. Conclusions</b> . . . . .	30
<b>References</b> . . . . .	31

## **Abstract**

## List of Tables

2.1	Analysis of variance results exploring species-specific effects of light availability, nitrogen fertilization, and their interactions on carbon costs to acquire nitrogen, whole-plant nitrogen biomass, and root carbon biomass . . . . .	11
2.2	Analysis of variance results exploring effects of light availability, nitrogen fertilization, and their interactions on <i>G. max</i> root nodule biomass and the ratio of root nodule biomass to root biomass* . .	18
2.3	Slopes of the regression line describing the relationship between each dependent variable and nitrogen fertilization at each light level*	19

## List of Figures

2.1	Relationships between soil nitrogen fertilization and light availability on carbon costs to acquire nitrogen in <i>G. hirsutum</i> and <i>G. max</i>	12
2.2	Relationships between soil nitrogen fertilization and light availability on whole-plant nitrogen biomass in <i>G. hirsutum</i> and <i>G. max</i>	14
2.3	Relationships between soil nitrogen fertilization and light availability on root carbon biomass in <i>G. hirsutum</i> and <i>G. max</i>	16
2.4	Effects of shade cover and nitrogen fertilization on root nodule biomass and the ratio of root nodule biomass to root biomass in <i>G. max</i>	20

**1**

**Chapter 1**

**2**

**Introduction**



3

## Chapter 2

4

5

6

# Structural carbon costs to acquire nitrogen are determined by nitrogen and light availability in two species with different nitrogen acquisition strategies

7

## 2.1 Introduction

8

9

10

11

12

13

14

15

16

17

18

19

20

21

22

23

24

25

26

Carbon and nitrogen cycles are tightly coupled in terrestrial ecosystems. This tight coupling influences photosynthesis (Walker et al. 2014; Rogers et al. 2017), net primary productivity (LeBauer and Treseder 2008; Thomas et al. 2013), decomposition (Cornwell et al. 2008; Bonan et al. 2013; Sulman et al. 2019), and plant resource competition (Gill and Finzi 2016; Xu-Ri and Prentice 2017). Terrestrial biosphere models are beginning to include connected carbon and nitrogen cycles to improve the realism of their simulations (Fisher et al. 2010; ?; Wieder et al. 2015; Shi et al. 2016; Zhu et al. 2019). Simulations from these models indicate that coupling carbon and nitrogen cycles can drastically influence future biosphere-atmosphere feedbacks under global change, such as elevated carbon dioxide or nitrogen deposition (Thornton et al. 2007; Goll et al. 2012; Wieder et al. 2015; Wieder et al. 2019). Nonetheless, there are still limitations in our quantitative understanding of connected carbon and nitrogen dynamics (Thomas et al. 2015; Meyerholt et al. 2016; Rogers et al. 2017; Exbrayat et al. 2018; Shi et al. 2019), forcing models to make potentially unreliable assumptions.

Plant nitrogen acquisition is a process in terrestrial ecosystems by which carbon and nitrogen are tightly coupled (Vitousek and Howarth 1991; Delaire et al. 2005; ?). Plants must allocate photosynthetically derived carbon below-ground to produce and maintain root systems or exchange with symbiotic soil

microbes in order to acquire nitrogen (Högberg et al. 2008; Högberg et al. 2010). Thus, plants have an inherent carbon cost associated with acquiring nitrogen, which can include both direct energetic costs associated with nitrogen acquisition and indirect costs associated with building structures that support nitrogen acquisition (Gutschick 1981; Rastetter et al. 2001; Vitousek et al. 2002; Menge et al. 2008). Model simulations (Fisher et al. 2010; ?; Shi et al. 2019; Allen et al. 2020) and meta-analyses (Terrer et al. 2018) suggest that these carbon costs vary between species, particularly those with different nitrogen acquisition strategies. For example, simulations using iterations of the Fixation and Uptake of Nitrogen (FUN) model indicate that species that acquire nitrogen from non-symbiotic active uptake pathways (e.g. mass flow) generally have larger carbon costs to acquire nitrogen than species that acquire nitrogen through symbiotic associations with nitrogen-fixing bacteria (?; Allen et al. 2020).

Carbon costs to acquire nitrogen likely vary in response to changes in soil nitrogen availability. For example, if the primary mode of nitrogen acquisition is through non-symbiotic active uptake, then nitrogen availability could decrease carbon costs to acquire nitrogen as a result of increased per-root nitrogen uptake (Franklin et al. 2009; Wang et al. 2018). However, if the primary mode of nitrogen acquisition is through symbiotic active uptake, then nitrogen availability may incur additional carbon costs to acquire nitrogen if it causes microbial symbionts to shift toward parasitism along the parasitism–mutualism continuum (Johnson et al. 1997; Hoek et al. 2016; Friel and Friesen 2019) or if it reduces the nitrogen acquisition capacity of a microbial symbiont (van Diepen et al. 2007; Soudzilovskaia et al. 2015; Muñoz et al. 2016). Species may respond to shifts in

soil nitrogen availability by switching their primary mode of nitrogen acquisition to a strategy with lower carbon costs to acquire nitrogen in order to maximize the magnitude of nitrogen acquired from a belowground carbon investment and outcompete other individuals for soil resources (Rastetter et al. 2001; Menge et al. 2008).

Environmental conditions that affect demand to acquire nitrogen to support new and existing tissues could also be a source of variance in plant carbon costs to acquire nitrogen. For example, an increase in plant nitrogen demand could increase carbon costs to acquire nitrogen if this increases the carbon that must be allocated belowground to acquire a proportional amount of nitrogen (Kulmatiski et al. 2017; Noyce et al. 2019). This could be driven by a temporary state of diminishing return associated with investing carbon toward building and maintaining structures that are necessary to support enhanced nitrogen uptake, such as fine roots (Matamala and Schlesinger 2000; Norby et al. 2004; Arndal et al. 2018), mycorrhizal hyphae (Saleh et al. 2020), or root nodules (Parvin et al. 2020). Alternatively, if the environmental factor that increases plant nitrogen demand causes nitrogen to become more limiting in the system (e.g. atmospheric CO<sub>2</sub>; Luo et al. (2004), LeBauer and Treseder (2008), Vitousek et al. (2010), Liang et al. (2016)), species might switch their primary mode of nitrogen acquisition to a strategy with lower relative carbon costs to acquire nitrogen in order to gain a competitive advantage over species with either different or more limited modes of nitrogen acquisition (Ainsworth and Long 2005; Taylor and Menge 2018).

Using a plant economics approach, we examined the influence of plant nitrogen demand and soil nitrogen availability on plant carbon costs to acquire

nitrogen. This was done by growing a species capable of forming associations with nitrogen-fixing bacteria (*Glycine max* L. (Merr)) and a species not capable of forming these associations (*Gossypium hirsutum* L.) under four levels of light availability (plant nitrogen demand proxy) and four levels of soil nitrogen fertilization (soil nitrogen availability proxy) in a full-factorial, controlled greenhouse experiment. We used this experimental set-up to test the following hypotheses:

1. An increase in plant nitrogen demand due to increasing light availability will increase carbon costs to acquire nitrogen through a proportionally larger increase in belowground carbon than whole-plant nitrogen acquisition. This will be the result of an increased investment of carbon toward belowground structures that support enhanced nitrogen uptake, but at a lower nitrogen return.
2. An increase in soil nitrogen availability will decrease carbon costs to acquire nitrogen as a result of increased per root nitrogen uptake in *G. hirsutum*. However, soil nitrogen availability will not affect carbon costs to acquire nitrogen in *G. max* because of the already high return of nitrogen supplied through nitrogen fixation.

## 2.2 Methods

### 2.2.1 *Experiment setup*

*Gossypium hirsutum* and *G. max* were planted in individual 3 liter pots (NS-300; Nursery Supplies, Orange, CA, USA) containing a 3:1 mix of unfertilized potting mix (Sungro Sunshine Mix #2, Agawam, MA, USA) to native soil

97 extracted from an agricultural field most recently planted with *G. max* at the  
98 USDA-ARS Laboratory in Lubbock, TX, USA (33.59°N, -101.90°W). The field  
99 soil was classified as Amarillo fine sandy loam (75% sand, 10% silt, 15% clay).  
100 Upon planting, all *G. max* pots were inoculated with *Bradyrhizobium japonicum*  
101 (Verdesian N-Dure™ Soybean, Cary, NC, USA) to stimulate root nodulation. In-  
102 dividuals of both species were grown under similar, unshaded, ambient greenhouse  
103 conditions for 2 weeks to germinate and begin vegetative growth. Three blocks  
104 were set up in the greenhouse, each containing four light treatments created us-  
105 ing shade cloth that reduced incoming radiation by either 0 (full sun), 30, 50,  
106 or 80%. Two weeks post-germination, individuals were randomly placed in the  
107 four light treatments in each block. Individuals received one of four nitrogen fer-  
108 tilization doses as 100ml of a modified Hoagland solution (Hoagland and Arnon  
109 1950) equivalent to either 0, 70, 210, or 630 ppm N twice per week within each  
110 light treatment. Nitrogen fertilization doses were received as topical agents to  
111 the soil surface. Each Hoagland solution was modified to keep concentrations of  
112 other macro- and micronutrients equivalent (Supplementary Table S1). Plants  
113 were routinely well watered to eliminate water stress.

#### 114 2.2.2 *Plant measurements and calculations*

115 Each individual was harvested after 5 weeks of treatment, and biomass  
116 was separated by organ type (leaves, stems, and roots). Nodules on *G. max*  
117 roots were also harvested. With the exception of the 0% shade cover and 630  
118 ppm N treatment combination, all treatment combinations in both species had  
119 lower average dry biomass:pot volume ratios than the 1:1 ratio recommended by

120 Poorter et al. (2012) to minimize the likelihood of pot volume-induced growth  
 121 limitation (Supplementary Tables S2, S3; Supplementary Fig. S1). All harvested  
 122 material was dried, weighed, and ground by organ type. Carbon and nitrogen  
 123 content ( $\text{g g}^{-1}$ ) was determined by subsampling from ground and homogenized  
 124 biomass of each organ type using an elemental analyzer (Costech 4010; Costech,  
 125 Inc., Valencia, CA, USA). We scaled these values to total leaf, stem, and root  
 126 carbon and nitrogen biomass (g) by multiplying dry biomass of each organ type  
 127 by carbon or nitrogen content of each corresponding organ type. Whole-plant  
 128 nitrogen biomass (g) was calculated as the sum of total leaf (g), stem (g), and  
 129 root (g) nitrogen biomass. Root nodule carbon biomass was not included in the  
 130 calculation of root carbon biomass; however, relative plant investment toward root  
 131 or root nodule standing stock was estimated as the ratio of root biomass to root  
 132 nodule biomass ( $\text{g g}^{-1}$ ), following similar metrics to those adopted by Dovrat et al.  
 133 (2018) and Dovrat et al. (2020).

134 Carbon costs to acquire nitrogen ( $\text{gC gN}^{-1}$ ) were estimated as the ratio of  
 135 total root carbon biomass (gC) to whole-plant nitrogen biomass (gN). This cal-  
 136 culation quantifies the relationship between carbon spent on nitrogen acquisition  
 137 and whole-plant nitrogen acquisition by using root carbon biomass as a proxy for  
 138 estimating the magnitude of carbon allocated toward nitrogen acquisition. This  
 139 calculation therefore assumes that the magnitude of root carbon standing stock is  
 140 proportional to carbon transferred to root nodules or mycorrhizae, or lost through  
 141 root exudation or turnover. This assumption has been supported in species that  
 142 associate with ectomycorrhizal fungi (Hobbie 2006; Hobbie and Hobbie 2008), but  
 143 is less clear in species that acquire nitrogen through non-symbiotic active uptake

or symbiotic nitrogen fixation. It is also unclear whether relationships between root carbon standing stock and carbon transfer to root nodules are similar in magnitude to carbon lost through exudation or when allocated toward other active uptake pathways. Thus, because of the way we performed our measurements, our proximal values of carbon costs to acquire nitrogen are underestimates.

### 2.2.3 *Statistical analyses*

We explored the effects of light and nitrogen availability on carbon costs to acquire nitrogen using separate linear mixed-effects models for each species. Models included shade cover, nitrogen fertilization, and interactions between shade cover and nitrogen fertilization as continuous fixed effects, and also included block as a random intercept term. Three separate models for each species were built with this independent variable structure for three different dependent variables: (i) carbon costs to acquire nitrogen ( $\text{gC gN}^{-1}$ ); (ii) whole-plant nitrogen biomass (denominator of carbon cost to acquire nitrogen;  $\text{gN}$ ); and (iii) root carbon biomass (numerator of carbon cost to acquire nitrogen;  $\text{gC}$ ). We constructed two additional models for *G. max* with the same model structure described above to investigate the effects of light availability and nitrogen fertilization on root nodule biomass (g) and the ratio of root nodule biomass to root biomass (unitless).

We used Shapiro–Wilk tests of normality to determine whether species-specific linear mixed-effects model residuals followed a normal distribution. None of our models satisfied residual normality assumptions when models were fit using untransformed data (Shapiro–Wilk:  $P < 0.05$  in all cases). We attempted to satisfy residual normality assumptions by first fitting models using dependent variables

that were natural-log transformed. If residual normality assumptions were still not met (Shapiro–Wilk:  $P < 0.05$ ), then models were fit using dependent variables that were square root transformed. All residual normality assumptions were satisfied when models were fit with either a natural-log or square root transformation (Shapiro–Wilk:  $P > 0.05$  in all cases). Specifically, we natural-log transformed *G. hirsutum* carbon costs to acquire nitrogen and *G. hirsutum* whole-plant nitrogen biomass. We also square root transformed *G. max* carbon costs to acquire nitrogen, *G. max* whole-plant nitrogen biomass, root carbon biomass in both species, *G. max* root nodule biomass, and the *G. max* ratio of root nodule biomass to root biomass. We used the ‘lmer’ function in the ‘lme4’ R package (Bates et al. 2015) to fit each model and the ‘Anova’ function in the ‘car’ R package (Fox and Weisberg 2019) to calculate Wald’s  $\chi^2$  to determine the significance ( $\alpha = 0.05$ ) of each fixed effect coefficient. Finally, we used the ‘emmeans’ R package (Lenth 2019) to conduct post-hoc comparisons of our treatment combinations using Tukey’s tests. Degrees of freedom for all Tukey’s tests were approximated using the Kenward–Roger approach (Kenward and Roger 1997). All analyses and plots were conducted in R version 4.0.1 (R Core Team 2021).

## 2.3 Results

### 2.3.1 Carbon costs to acquire nitrogen

Carbon costs to acquire nitrogen in *G. hirsutum* increased with increasing light availability ( $P < 0.001$ ; Table 1; Fig. 1) and decreased with increasing nitrogen fertilization ( $P < 0.001$ ; Table 1; Fig. 1). There was no interaction between light availability and nitrogen fertilization ( $P = 0.486$ ; Table 2.1; Fig. 2.1).



**190** Carbon costs to acquire nitrogen in *G. max* also increased with increasing  
**191** light availability ( $P < 0.001$ ; Table 1; Fig. 1) and decreased with increasing nitrogen  
**192** fertilization ( $P < 0.001$ ; Table 1; Fig. 1). There was no interaction between light  
**193** availability and nitrogen fertilization ( $P = 0.261$ ; Table 2.1; Fig. 2.1).

**Table 2.1.** Analysis of variance results exploring species-specific effects of light availability, nitrogen fertilization, and their interactions on carbon costs to acquire nitrogen, whole-plant nitrogen biomass, and root carbon biomass

		Carbon costs to acquire nitrogen			Whole-plant nitrogen biomass			Root carbon biomass		
	df	Coefficient	$\chi^2$	<i>P</i> -value	Coefficient	$\chi^2$	<i>P</i> -value	Coefficient	$\chi^2$	<i>P</i> -value
<i>G. hirsutum</i>										
Intercept		1.594	-	-	-3.232	-	-	0.432	-	-
Light (L)	1	-1.09E-02	56.494	<b>&lt;0.001</b>	-6.41E-03	91.275	<b>&lt;0.001</b>	-2.62E-03	169.608	<b>&lt;0.001</b>
Nitrogen (N)	1	-1.34E-03	54.925	<b>&lt;0.001</b>	1.83E-03	118.784	<b>&lt;0.001</b>	1.15E-04	2.901	<i>0.089</i>
L*N	1	3.88E-06	0.485	0.486	-1.34E-05	10.721	<b>0.001</b>	-1.67E-06	3.140	<i>0.076</i>
<i>G. max</i>										
Intercept		1.877	-	-	0.239	-	-	0.438	-	-
Light (L)	1	-7.67E-03	174.156	<b>&lt;0.001</b>	-6.72E-04	39.799	<b>&lt;0.001</b>	-2.55E-03	194.548	<b>&lt;0.001</b>
Nitrogen (N)	1	-2.35E-04	21.948	<b>&lt;0.001</b>	1.55E-04	70.771	<b>&lt;0.001</b>	2.52E-04	19.458	<b>&lt;0.001</b>
L*N	1	-2.89E-06	1.262	0.261	-6.32E-07	1.435	0.231	-3.16E-06	10.803	<b>0.001</b>

\*Significance determined using Wald's  $\chi^2$  tests ( $P=0.05$ ).  $P$ -values<0.05 are in bold and marginally insignificant  $P$ -values between 0.050 and 0.100 are italicized. Negative coefficients for light treatments indicate a positive effect of increasing light availability on all response variables, as light availability is treated as percent shade cover in all linear mixed-effects models.

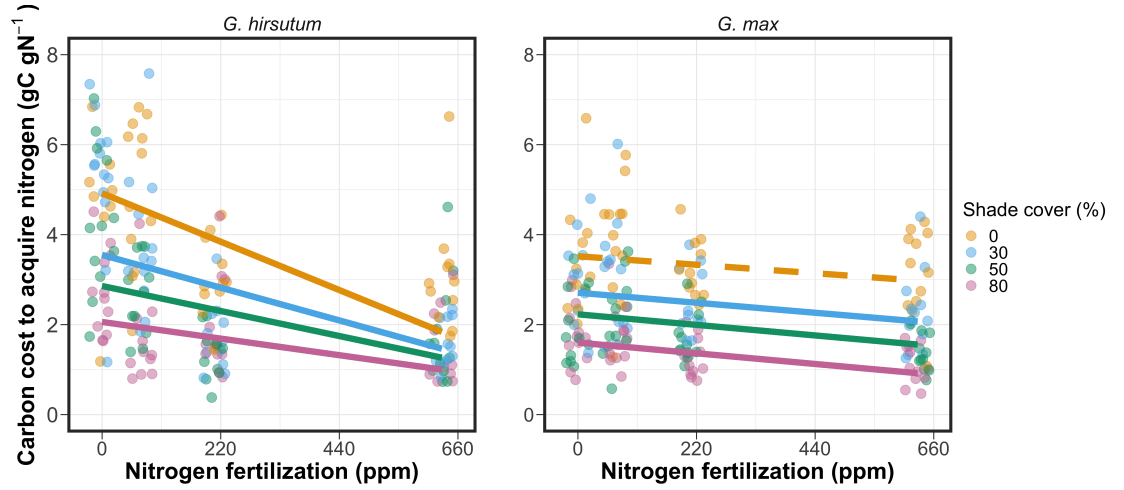


**Figure 2.1.** Relationships between soil nutrient fertilization and light availability on carbon costs to acquire nitrogen in *G. hirsutum* and *G. max*. Nitrogen fertilization treatments are represented on the x-axis. Shade cover treatments are represented through colored points and trendlines. Trendlines were created by back-transforming marginal mean slopes and intercepts from species-specific linear mixed-effects models. These values were calculated using the ‘emtrends’ and ‘emmeans’ functions in the ‘emmeans’ R package (Lenth, 2019). Points are jittered for visibility. Yellow points and trendlines represent the 0% shade cover treatment, blue points and trendlines represent the 30% shade cover treatment, green points and trendlines represent the 50% shade cover treatment, and purple points and trendlines represent the 80% shade cover treatment. Solid trendlines indicate slopes that are significantly different from zero (Tukey:  $P < 0.05$ ), while dashed trendlines indicate slopes that are not statistically different from zero.

**194** 2.3.2 *Whole plant nitrogen biomass*

**195** Whole-plant nitrogen biomass in *G. hirsutum* was driven by an interaction  
**196** between light availability and nitrogen fertilization ( $P=0.001$ ; Table 1; Fig. 2).  
**197** This interaction indicated a greater stimulation of whole-plant nitrogen biomass  
**198** by nitrogen fertilization as light levels increased (Table 2.1; Fig. 2.2).

**199** Whole-plant nitrogen biomass in *G. max* increased with increasing light  
**200** availability ( $P<0.001$ ) and nitrogen fertilization ( $P<0.001$ ), with no interaction  
**201** between light availability and nitrogen fertilization ( $P=0.231$ ; Table 2.1; Fig. 2.2).

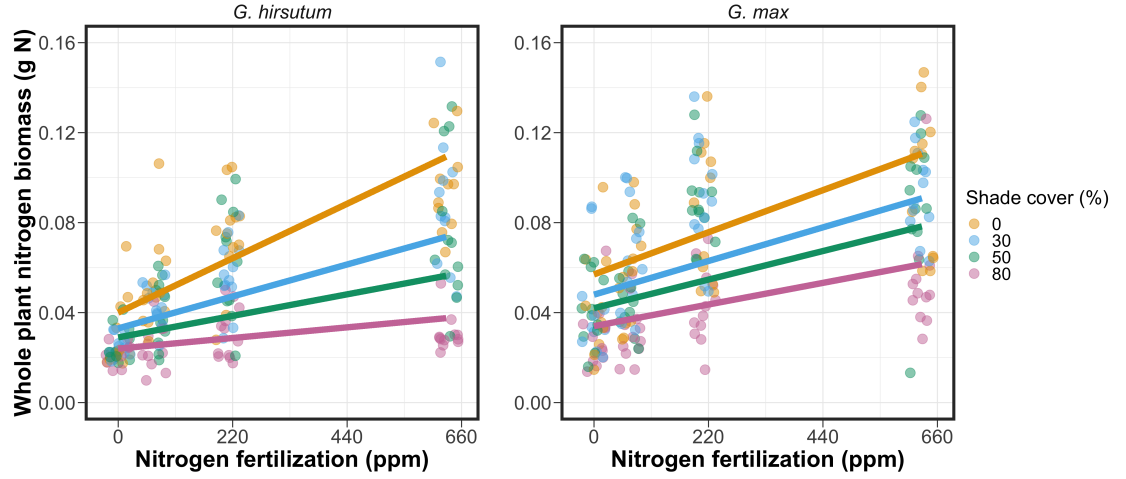


**Figure 2.2.** Relationships between soil nutrient fertilization and light availability on whole-plant nitrogen biomass in *G. hirsutum* and *G. max*. Whole-plant nitrogen biomass is the denominator of the carbon cost to acquire nitrogen calculation. Nitrogen fertilization treatments are represented on the x-axis. Shade cover treatments are represented through colored points and trendlines. Trendlines were created by back-transforming marginal mean slopes and intercepts from species-specific linear mixed-effects models. These values were calculated using the ‘emtrends’ and ‘emmeans’ functions in the ‘emmeans’ R package (Lenth 2019). Points are jittered for visibility. Yellow points and trendlines represent the 0% shade cover treatment, blue points and trendlines represent the 30% shade cover treatment, green points and trendlines represent the 50% shade cover treatment, and purple points and trendlines represent the 80% shade cover treatment. Solid trendlines indicate slopes that are significantly different from zero (Tukey:  $P < 0.05$ ), while dashed trendlines indicate slopes that are not statistically different from zero.

### 202 2.3.3 *Root carbon biomass*

203           Root carbon biomass in *G. hirsutum* significantly increased with increasing  
 204 light availability ( $P < 0.001$ ; Table 1; Fig. 3) and marginally increased with nitro-  
 205 gen fertilization ( $P = 0.089$ ; Table 1; Fig. 3). There was also a marginal interaction  
 206 between light availability and nitrogen fertilization ( $P = 0.076$ ; Table 1), driven by  
 207 an increase in the positive response of root carbon biomass to increasing nitrogen  
 208 fertilization as light availability increased. This resulted in significantly positive  
 209 trends between root carbon biomass and nitrogen fertilization in the two highest  
 210 light treatments (Tukey:  $P < 0.05$  in both cases; Table 2.3; Fig. 2.3) and no effect  
 211 of nitrogen fertilization in the two lowest light treatments (Tukey:  $P > 0.05$  in both  
 212 cases; Table 3; Fig. 3).

213           There was an interaction between light availability and nitrogen fertiliza-  
 214 tion on root carbon biomass in *G. max* ( $P = 0.001$ ; Table 1; Fig. 3). Post-hoc  
 215 analyses indicated that the positive effects of nitrogen fertilization on *G. max*  
 216 root carbon biomass increased with increasing light availability (Table 3; Fig.  
 217 3). There were also positive individual effects of increasing nitrogen fertilization  
 218 ( $P < 0.001$ ) and light availability ( $P < 0.001$ ) on *G. max* root carbon biomass (Table  
 219 1; Fig. 2.3).

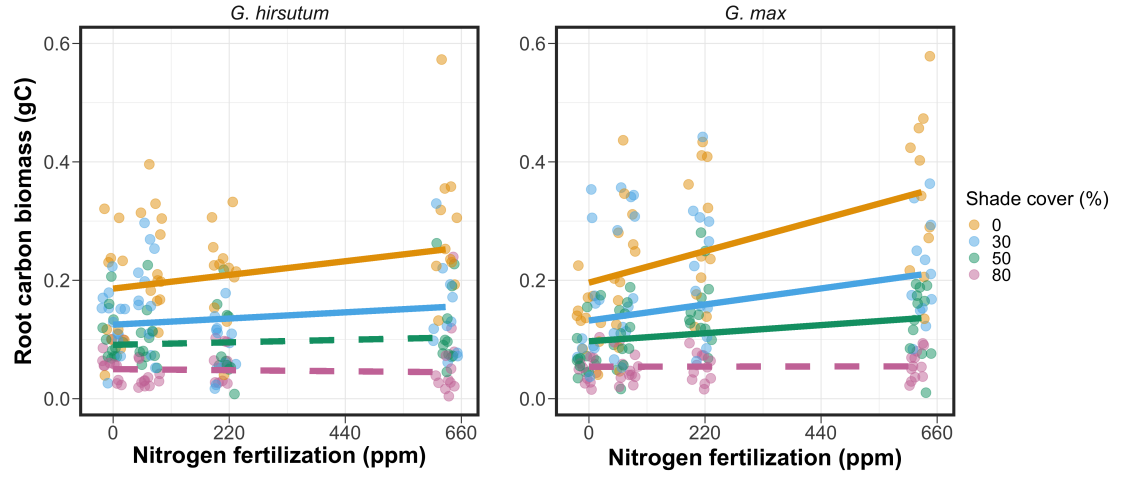


**Figure 2.3.** Relationships between soil nutrient fertilization and light availability on root carbon biomass in *G. hirsutum* and *G. max*. Root carbon biomass is the numerator of the carbon cost to acquire nitrogen calculation. Nitrogen fertilization treatments are represented on the x-axis. Shade cover treatments are represented through colored points and trendlines. Trendlines were created by back-transforming marginal mean slopes and intercepts from species-specific linear mixed-effects models. These values were calculated using the ‘emtrends’ and ‘emmeans’ functions in the ‘emmeans’ R package (Lenth 2019). Points are jittered for visibility. Yellow points and trendlines represent the 0% shade cover treatment, blue points and trendlines represent the 30% shade cover treatment, green points and trendlines represent the 50% shade cover treatment, and purple points and trendlines represent the 80% shade cover treatment. Solid trendlines indicate slopes that are significantly different from zero (Tukey:  $P < 0.05$ ), while dashed trendlines indicate slopes that are not statistically different from zero.

**220** 2.3.4 *Root nodule biomass*

**221** Root nodule biomass in *G. max* increased with increasing light availability  
**222** ( $P < 0.001$ ; Table 2; Fig. 4A) and decreased with increasing nitrogen fertilization  
**223** ( $P < 0.001$ ; Table 2; Fig. 4A). There was no interaction between nitrogen fertiliza-  
**224** tion and light availability ( $P = 0.133$ ; Table 2; Fig. 4A). The ratio of root nodule  
**225** biomass to root biomass did not change in response to light availability ( $P = 0.481$ ;  
**226** Table 2; Fig. 4B) but decreased with increasing nitrogen fertilization ( $P < 0.001$ ;  
**227** Table 2; Fig. 4B). There was no interaction between nitrogen fertilization and  
**228** light availability on the ratio of root nodule biomass to root biomass ( $P = 0.621$ ;  
**229** Table 2; Fig. 4B).



**Table 2.2.** Analysis of variance results exploring effects of light availability, nitrogen fertilization, and their interactions on *G. max* root nodule biomass and the ratio of root nodule biomass to root biomass\*

	Nodule biomass				Nodule biomass: root biomass		
	df	Coefficient	$\chi^2$	<i>P</i> -value	Coefficient	$\chi^2$	<i>P</i> -value
Intercept		0.302	-	-	0.448	-	-
Light (L)	1	-1.81E-03	72.964	<b>&lt;0.001</b>	-8.76E-05	0.496	0.481
Nitrogen (N)	1	-2.83E-04	115.377	<b>&lt;0.001</b>	-5.09E-04	156.476	<b>&lt;0.001</b>
L*N	1	1.14E-06	2.226	0.133	-7.30E-07	0.244	0.621

\*Significance determined using Wald's  $\chi^2$  tests ( $\alpha=0.05$ ). *P*-values less than 0.05 are in bold. Negative coefficients for light treatments indicate a positive effect of increasing light availability on all response variables, as light availability is treated as percent shade cover in all linear mixed-effects models. Root nodule biomass and nodule biomass: root biomass models were only constructed for *G. max* because *G. hirsutum* was not inoculated with *B. japonicum* and is not capable of forming root nodules.

**Table 2.3.** Slopes of the regression line describing the relationship between each dependent variable and nitrogen fertilization at each light level\*

Shade cover	Carbon cost to acquire nitrogen	Whole-plant nitrogen biomass	Root carbon biomass	Root nodule biomass	Nodule biomass root biomass
<i>G. hirsutum</i>					
0%	<b>-1.34E-03<sup>a</sup></b>	<b>1.83E-03<sup>a</sup></b>	<b>1.15E-04<sup>b</sup></b>	-	-
30%	<b>-1.22E-03<sup>a</sup></b>	<b>1.43E-03<sup>a</sup></b>	<b>1.17E-04<sup>b</sup></b>	-	-
50%	<b>-1.14E-03<sup>a</sup></b>	<b>1.17E-03<sup>a</sup></b>	3.12E-05 <sup>b</sup>	-	-
80%	<b>-1.02E-03<sup>a</sup></b>	<b>7.66E-04<sup>a</sup></b>	-1.89E-06 <sup>b</sup>	-	-
<i>G. max</i>					
0%	-2.35E-04 <sup>b</sup>	<b>1.55E-05<sup>b</sup></b>	<b>2.51E-04<sup>b</sup></b>	<b>-2.83E-04<sup>b</sup></b>	<b>-5.09E-04<sup>b</sup></b>
30%	<b>-3.22E-04<sup>b</sup></b>	<b>1.35E-05<sup>b</sup></b>	<b>1.57E-04<sup>b</sup></b>	<b>-2.49E-04<sup>b</sup></b>	<b>-5.31E-04<sup>b</sup></b>
50%	<b>-3.80E-04<sup>b</sup></b>	<b>1.23E-05<sup>b</sup></b>	<b>9.37E-05<sup>b</sup></b>	<b>-2.26E-04<sup>b</sup></b>	<b>-5.45E-04<sup>b</sup></b>
80%	<b>-4.66E-04<sup>b</sup></b>	<b>1.04E-05<sup>b</sup></b>	-9.95E-07 <sup>b</sup>	<b>-1.92E-04<sup>b</sup></b>	<b>-5.67E-04<sup>b</sup></b>

\*Slopes represent estimated marginal mean slopes from linear mixed-effects models described in the Methods. Slopes were calculated using the ‘emmeans’ R package (Lenth 2019). Superscripts indicate slopes fit to natural-log (<sup>a</sup>) or square root (<sup>b</sup>) transformed data. Slopes statistically different from zero (Tukey:  $P < 0.05$ ) are indicated in bold. Marginally significant slopes (Tukey:  $0.05 < P < 0.1$ ) are italicized.

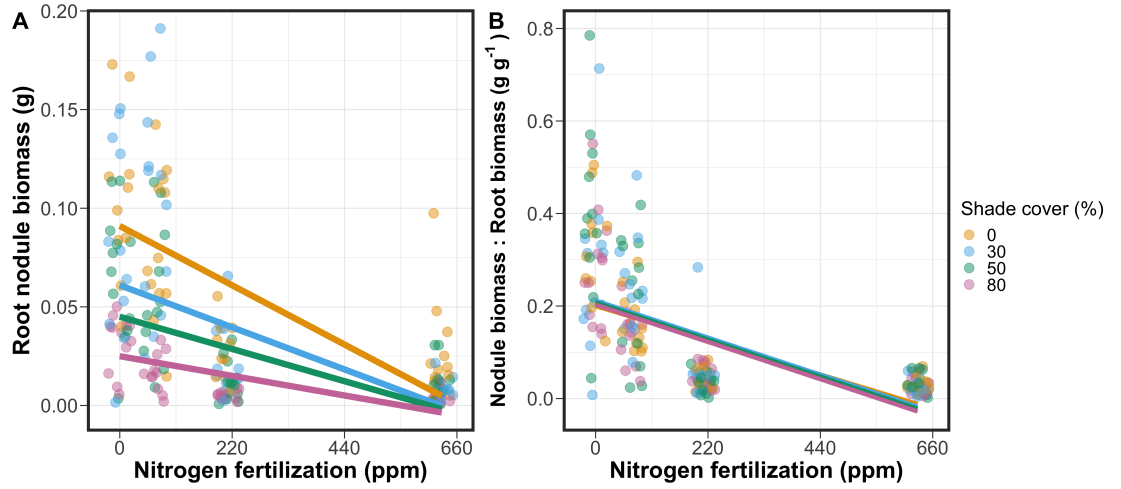


**Figure 2.4.** Effects of shade cover and nitrogen fertilization on root nodule biomass (A) and the ratio of root nodule biomass to root biomass (B) in *G. max*. Nitrogen fertilization treatments are represented on the x-axis. Shade cover treatments are represented through colored points and trendlines. Trendlines were created by back-transforming marginal mean slopes and intercepts from species-specific linear mixed-effects models. These values were calculated using the ‘emtrends’ and ‘emmeans’ functions in the ‘emmeans’ R package (Lenth, 2019). Points are jittered for visibility. Yellow points and trendlines represent the 0% shade cover treatment, blue points and trendlines represent the 30% shade cover treatment, green points and trendlines represent the 50% shade cover treatment, and purple points and trendlines represent the 80% shade cover treatment. Solid trendlines indicate slopes that are significantly different from zero (Tukey:  $P < 0.05$ ), while dashed trendlines indicate slopes that are not statistically different from zero.

## 230 2.4 Discussion

231        In this chapter, we determined the effects of light availability and soil ni-  
 232 trogen fertilization on root mass carbon costs to acquire nitrogen in *G. hirsutum*  
 233 and *G. max*. In support of our hypotheses, we found that carbon costs to acquire  
 234 nitrogen generally increased with increasing light availability and decreased with  
 235 increasing soil nitrogen fertilization in both species. These findings suggest that  
 236 carbon costs to acquire nitrogen are determined by factors that influence plant  
 237 nitrogen demand and soil nitrogen availability. In contrast to our second hypothe-  
 238 sis, root nodulation data suggested that *G. max* and *G. hirsutum* achieved similar  
 239 directional carbon cost responses to nitrogen fertilization despite a likely shift in  
 240 *G. max* allocation from nodulation to root biomass along the nitrogen fertilization  
 241 gradient (Fig. 2.4B).

242        Both *G. max* and *G. hirsutum* experienced an increase in carbon costs to  
 243 acquire nitrogen due to increasing light availability. These patterns were driven by  
 244 a larger increase in root carbon biomass than whole-plant nitrogen biomass. In-  
 245 creases in root carbon biomass due to factors that increase plant nitrogen demand  
 246 are a commonly observed pattern, as carbon allocated belowground provides sub-  
 247 strate needed to produce and maintain structures that satisfy aboveground plant  
 248 nitrogen demand (Nadelhoffer and Raich 1992; Giardina et al. 2005; Raich et al.  
 249 2014). Our findings suggest that plants allocate relatively more carbon for acquir-  
 250 ing nitrogen when demand increases over short temporal scales, which may cause  
 251 a temporary state of diminishing return due to asynchrony between belowground  
 252 carbon and whole-plant nitrogen responses to plant nitrogen demand (Kulmatiski  
 253 et al. 2017; Noyce et al. 2019). These responses might be attributed to a temporal

lag associated with producing structures that enhance nitrogen acquisition. For example, fine roots (Matamala and Schlesinger 2000; Norby et al. 2004; Arndal et al. 2018) and root nodules (Parvin et al. 2020) take time to build and first require the construction of coarse roots. Thus, full nitrogen returns from these investments may not occur immediately (Kayler et al. 2010; Kayler et al. 2017), and may vary by species acquisition strategy. We speculate that increases in nitrogen acquisition from a given carbon investment may occur beyond the 5 week scope of this experiment. A similar study conducted over a longer temporal scale would address this.

Increasing soil nitrogen fertilization generally decreased carbon costs to acquire nitrogen in both species. These patterns were driven by a larger increase in whole-plant nitrogen biomass than root carbon biomass. In *G. hirsutum*, reductions in carbon costs to acquire nitrogen may have been due to an increase in per-root nitrogen uptake, allowing individuals to maximize the amount of nitrogen acquired from a belowground carbon investment. Interestingly, increased soil nitrogen fertilization increased whole-plant nitrogen biomass in *G. max* despite reductions in root nodule biomass that likely reduced the nitrogen-fixing capacity of *G. max* (Andersen et al. 2005; Muñoz et al. 2016). While reductions in root nodulation due to increased soil nitrogen availability are commonly observed (Gibson and Harper 1985; Fujikake et al. 2003), our responses were observed in tandem with increased root carbon biomass, implying that *G. max* shifted relative carbon allocation from nitrogen fixation to soil nitrogen acquisition (Markham and Zekveld 2007; Dovrat et al. 2020). This was likely because there was a reduction in the carbon cost advantage of acquiring fixed nitrogen relative to soil nitrogen, and

278 suggests that species capable of associating with symbiotic nitrogen-fixing bacte-  
279 ria shift their relative nitrogen acquisition pathway to optimize nitrogen uptake  
280 (Rastetter et al. 2001). Future studies should further investigate these patterns  
281 with a larger quantity of phylogenetically related species, or different varieties  
282 of a single species that differ in their ability to form associations with symbiotic  
283 nitrogen-fixing bacteria to more directly test the impact of nitrogen fixation on  
284 the patterns observed in this study.

285         Carbon costs to acquire nitrogen are subsumed in the general discussion of  
286 economic analogies to plant resource uptake (Bloom et al. 1985; Rastetter et al.  
287 2001; Vitousek et al. 2002; Phillips et al. 2013; Terrer et al. 2018; Henneron  
288 et al. 2020). Despite this, terrestrial biosphere models rarely include these carbon  
289 costs within their framework for predicting plant nitrogen uptake. There is cur-  
290 rently one plant resource uptake model, FUN, that quantitatively predicts carbon  
291 costs to acquire nitrogen within a framework for predicting plant nitrogen uptake  
292 for different nitrogen acquisition strategies (Fisher et al. 2010; ?). Iterations of  
293 FUN are currently coupled to two terrestrial biosphere models: the Community  
294 Land Model 5.0 and the Joint UK Land Environment Simulator (Shi et al. 2016;  
295 Lawrence et al. 2019; Clark et al. 2011). Recent work suggests that coupling  
296 FUN to CLM 5.0 caused a large overprediction of plant nitrogen uptake associ-  
297 ated with nitrogen fixation (Davies-Barnard et al. 2020). Thus, empirical data  
298 from manipulative experiments that explicitly quantify carbon costs to acquire  
299 nitrogen in species capable of associating with nitrogen-fixing bacteria across dif-  
300 ferent environmental contexts is an important step toward identifying potential  
301 biases in models such as FUN.

Our findings broadly support the FUN formulation of carbon costs to acquire nitrogen in response to soil nitrogen availability. FUN calculates carbon costs to acquire nitrogen based on the sum of carbon costs to acquire nitrogen via nitrogen fixation, mycorrhizal active uptake, non-mycorrhizal active uptake, and retranslocation (Fisher et al. 2010; ?). Carbon costs to acquire nitrogen via mycorrhizal or non-mycorrhizal active uptake pathways are derived as a function of nitrogen availability, root biomass, and two parameterized values based on nitrogen acquisition strategy (?). Due to this, FUN simulates a net decrease in carbon costs to acquire nitrogen with increasing nitrogen availability for mycorrhizal and non-mycorrhizal active uptake pathways, assuming constant root biomass. This was a pattern we observed in *G. hirsutum* regardless of light availability. In contrast, FUN would not simulate a net change in carbon costs to acquire nitrogen via nitrogen fixation due to nitrogen availability. This is because carbon costs to acquire nitrogen via nitrogen fixation are derived from a well-established function of soil temperature, which is independent of soil nitrogen availability (Houlton et al. 2008; Fisher et al. 2010). We observed a net reduction in carbon costs to acquire nitrogen in *G. max*, except when individuals were grown under 0% shade cover (Fig. 1). While a net reduction of carbon costs in response to nitrogen fertilization runs counter to nitrogen fixation carbon costs simulated by FUN, these patterns were likely because *G. max* individuals switched their primary mode of nitrogen acquisition from symbiotic nitrogen fixation to a non-symbiotic active uptake pathway (Fig. 4B).

It should be noted that the metric used in this study to determine carbon costs to acquire nitrogen has several limitations. Most notably, this metric uses

326 root carbon biomass as a proxy for estimating the amount of carbon spent on  
 327 nitrogen acquisition. While it is true that most carbon allocated belowground  
 328 has at least an indirect structural role in acquiring soil resources, it remains un-  
 329 clear whether this assumption holds true for species that acquire nitrogen via  
 330 symbiotic nitrogen fixation. We also cannot quantify carbon lost through root  
 331 exudates or root turnover, which may increase due to factors that increase plant  
 332 nitrogen demand (Tingey et al. 2000; Phillips et al. 2011), and can increase the  
 333 magnitude of available nitrogen from soil organic matter through priming effects  
 334 on soil microbial communities (Usselman et al. 2000; Bengtson et al. 2012). It  
 335 is also not clear whether these assumptions hold under all environmental condi-  
 336 tions, such as those that shift belowground carbon allocation toward a different  
 337 mode of nitrogen acquisition (Taylor and Menge 2018; Friel and Friesen 2019)  
 338 or between species with different acquisition strategies. In this study, increasing  
 339 soil nitrogen fertilization increased carbon investment to roots relative to carbon  
 340 transferred to root nodules (Fig. 4B). By assuming that carbon allocated to root  
 341 carbon was proportional to carbon allocated to root nodules across all treatment  
 342 combinations, these observed responses to soil nitrogen fertilization were likely  
 343 to be overestimated in *G. max*. We encourage future research to quantify these  
 344 carbon fates independently.

345         Researchers conducting pot experiments must carefully choose pot volume  
 346 to minimize the likelihood of pot volume-induced growth limitation (Poorter et al.  
 347 2012). Poorter et al. (2012) indicate that researchers are likely to avoid growth  
 348 limitations associated with pot volume if measurements are collected when the  
 349 plant biomass:pot volume ratio is less than 1 g L<sup>-1</sup>. In this experiment, all treat-



ment combinations in both species had biomass:pot volume ratios less than 1 g L<sup>-1</sup> except for *G. max* and *G. hirsutum* that were grown under 0% shade cover and had received 630 ppm N. Specifically, *G. max* and *G. hirsutum* had average respective biomass:pot volume ratios of  $1.24 \pm 0.07$  g L<sup>-1</sup> and  $1.34 \pm 0.13$  g L<sup>-1</sup>, when grown under 0% shade cover and received 630 ppm N (Supplementary Tables S2, S3; Supplementary Fig. S1). If growth in this treatment combination was limited by pot volume, then individuals may have had larger carbon costs to acquire nitrogen than would be expected if they were grown in larger pots. This pot volume induced growth limitation could cause a reduction in per-root nitrogen uptake associated with more densely packed roots, which could reduce the positive effect of nitrogen fertilization on whole-plant nitrogen biomass relative to root carbon biomass (Poorter et al. 2012).

Growth limitation associated with pot volume provides a possible explanation for the marginally insignificant effect of increasing nitrogen fertilization on *G. max* carbon costs to acquire nitrogen when grown under 0% shade cover (Table 3; Fig. 1). This is because the regression line describing the relationship between carbon costs to acquire nitrogen and nitrogen fertilization in *G. max* grown under 0% shade cover would have flattened if growth limitation had caused larger than expected carbon costs to acquire nitrogen in the 0% shade cover, 630 ppm N treatment combination. This may have been exacerbated by the fact that *G. max* likely shifted relative carbon allocation from nitrogen fixation to soil nitrogen acquisition, which could have increased the negative effect of more densely packed roots on nitrogen uptake. These patterns could have also occurred in *G. hirsutum* grown under 0% shade cover; however, there was no change in the effect of nitro-

374 gen fertilization on *G. hirsutum* carbon costs to acquire nitrogen grown under 0%  
 375 shade cover relative to other shade cover treatments. Regardless, the possibility  
 376 of growth limitation due to pot volume suggests that effects of increasing nitro-  
 377 gen fertilization on carbon costs to acquire nitrogen in both species grown under  
 378 0% shade cover could have been underestimated. Follow-up studies using a simi-  
 379 lar experimental design with a larger pot volume would be necessary in order to  
 380 determine whether these patterns were impacted by pot volume-induced growth  
 381 limitation.

382         In conclusion, this study provides empirical evidence that carbon costs to  
 383 acquire nitrogen are influenced by light availability and soil nitrogen fertilization  
 384 in a species capable of acquiring nitrogen via symbiotic nitrogen fixation and a  
 385 species not capable of forming such associations. We show that carbon costs to  
 386 acquire nitrogen generally increase with increasing light availability and decrease  
 387 with increasing nitrogen fertilization. This study provides important empirical  
 388 data needed to evaluate the formulation of carbon costs to acquire nitrogen in  
 389 terrestrial biosphere models, particularly carbon costs to acquire nitrogen that  
 390 are associated with symbiotic nitrogen fixation. Our findings broadly support  
 391 the general formulation of these carbon costs in the FUN biogeochemical model  
 392 in response to shifts in nitrogen availability. However, there is a need for future  
 393 studies to explicitly quantify carbon costs to acquire nitrogen under different en-  
 394 vironmental contexts, over longer temporal scales, and using larger selections of  
 395 phylogenetically related species. In addition, we suggest that future studies mini-  
 396 mize the limitations associated with the metric used here by explicitly measuring  
 397 belowground carbon fates independently.

398

## Chapter 3

399 **Soil nitrogen availability modifies leaf nitrogen economies in mature**  
 400 **temperate deciduous forests: a direct test of photosynthetic least-cost**  
 401 **theory**

### 402 3.1 Introduction

403       Photosynthesis represents the largest carbon flux between the atmosphere  
 404 and land surface (Masson-Delmotte et al. 2021), and plays a central role in biogeo-  
 405 chemical cycling at multiple spatial and temporal scales (Vitousek and Howarth  
 406 1991; LeBauer and Treseder 2008; Kaiser et al. 2015; Wieder et al. 2015). There-  
 407 fore, carbon and energy fluxes simulated by terrestrial biosphere models are sen-  
 408 sitive to the formulation of photosynthetic processes (Ziehn et al. 2011; Bonan  
 409 et al. 2011; Booth et al. 2012; Smith et al. 2016; Smith et al. 2017) and must  
 410 be represented using robust, empirically tested processes (Prentice et al. 2015;  
 411 Wieder et al. 2019). Current formulations of photosynthesis vary across terres-  
 412 trial biosphere models (Smith and Dukes 2013; Rogers et al. 2017), which causes  
 413 variation in modeled ecosystem processes (Knorr 2000; Knorr and Heimann 2001;  
 414 Bonan et al. 2011; Friedlingstein et al. 2014) and casts uncertainty on the ability  
 415 of these models to accurately predict terrestrial ecosystem responses and feed-  
 416 backs to global change (Zaehle et al. 2005; Schaefer et al. 2012; Davies-Barnard  
 417 et al. 2020)

418       Terrestrial biosphere models commonly represent C3 photosynthesis through  
 419 variants of the Farquhar et al. (1980) biochemical model (Smith and Dukes 2013;  
 420 Rogers 2014; Rogers et al. 2017). This well-tested photosynthesis model es-  
 421 timates leaf-level carbon assimilation, or photosynthetic capacity, as a function

of the maximum rate of Ribulose-1,5-bisphosphate carboxylase-oxygenase (Ru-  
 bisco) carboxylation ( $V_{\text{cmax}}$ ) and the maximum rate of Ribulose-1,5-bisphosphate  
 (RuBP) regeneration ( $J_{\text{max}}$ ; Farquhar et al., 1980). Many terrestrial biosphere  
 models predict these model inputs based on plant functional group specific linear  
 relationships between leaf nutrient content and  $V_{\text{cmax}}$  (Smith and Dukes 2013;  
 Rogers 2014; Rogers et al. 2017) under the tenet that a large fraction of leaf  
 nutrients, and nitrogen (N) in particular, are partitioned toward building and  
 maintaining enzymes that support photosynthetic capacity, such as Rubisco (Brix  
 1971; Gulmon and Chu 1981; Evans and Seemann 1989; Kattge et al. 2009;  
 Walker et al. 2014). Terrestrial biosphere models also predict leaf nutrient con-  
 tent from soil nutrient availability based on the assumption that increasing soil  
 nutrients generally increases leaf nutrients (Firn et al. 2019; Li et al. 2020; Liang  
 et al. 2020), which, in the case of nitrogen, generally corresponds with an increase  
 in photosynthetic processes (Li et al. 2020; Liang et al. 2020).

Recent work calls the generality of relationships between soil nutrient avail-  
 ability, leaf nutrient content, and photosynthetic capacity into question, suggest-  
 ing instead that leaf nutrients and photosynthetic capacity are better predicted as  
 an integrated product of aboveground climate, leaf traits, and soil nutrient avail-  
 ability, rather than soil nutrient availability alone (??; Firn et al. 2019; ??).  
 It has been reasoned that this result is because plants allocate added nutrients  
 to growth and storage rather than alterations in leaf chemistry (?), perhaps as a  
 result of nutrient limitation of primary productivity (LeBauer and Treseder 2008;  
 ?). Additionally, recent work suggests that relationships between leaf nutrient  
 content and photosynthesis vary across environments, and that the proportion

446 of leaf nutrient content allocated to photosynthetic tissue varies over space and  
447 time with plant acclimation and adaptation responses to light availability, vapor  
448 pressure deficit, soil pH, soil nutrient availability, and environmental factors that  
449 influence leaf mass per area (?; ?; ?; ?; ?; ?; ?). The use of linear relationships  
450 between leaf nutrient content and  $V_{\text{cmax}}$  to predict photosynthetic capacity, as  
451 commonly used in terrestrial biosphere models (Rogers 2014), is not capable of  
452 detecting such responses.

## 453 3.2 Methods

## 454 3.3 Results

**455**

**Chapter 4**

**456**

**Conclusions**

457

## References

- 458 Ainsworth, E. A. and S. P. Long (2005). What have we learned from 15 years of  
 459 free-air CO<sub>2</sub> enrichment (FACE)? A meta-analytic review of the responses  
 460 of photosynthesis, canopy properties and plant production to rising CO<sub>2</sub>.  
 461 *New Phytologist* 165(2), 351–372.
- 462 Allen, K., J. B. Fisher, R. P. Phillips, J. S. Powers, and E. R. Brzostek  
 463 (2020). Modeling the carbon cost of plant nitrogen and phosphorus up-  
 464 take across temperate and tropical forests. *Frontiers in Forests and Global*  
 465 *Change* 3(May), 1–12.
- 466 Andersen, M. K., H. Hauggaard-Nielsen, P. Ambus, and E. S. Jensen (2005,  
 467 jan). Biomass production, symbiotic nitrogen fixation and inorganic N use  
 468 in dual and tri-component annual intercrops. *Plant and Soil* 266(1-2), 273–  
 469 287.
- 470 Arndal, M. F., A. Tolver, K. S. Larsen, C. Beier, and I. K. Schmidt (2018). Fine  
 471 root growth and vertical distribution in response to elevated CO<sub>2</sub>, warming  
 472 and drought in a mixed heathland–grassland. *Ecosystems* 21(1), 15–30.
- 473 Bates, D., M. Mächler, B. Bolker, and S. Walker (2015). Fitting linear mixed-  
 474 effects models using lme4. *Journal of Statistical Software* 67(1), 1–48.
- 475 Bengtson, P., J. Barker, and S. J. Grayston (2012, aug). Evidence of a strong  
 476 coupling between root exudation, C and N availability, and stimulated SOM  
 477 decomposition caused by rhizosphere priming effects. *Ecology and Evolu-*  
 478 *tion* 2(8), 1843–1852.

- 479 Bloom, A. J., F. S. Chapin, and H. A. Mooney (1985, nov). Resource Limitation  
480 in Plants-An Economic Analogy. *Annual Review of Ecology and Systemat-*  
481 *ics* 16(1), 363–392.
- 482 Bonan, G. B., M. D. Hartman, W. J. Parton, and W. R. Wieder (2013, mar).  
483 Evaluating litter decomposition in earth system models with long-term lit-  
484 terbag experiments: an example using the Community Land Model version  
485 4 (CLM4). *Global Change Biology* 19(3), 957–974.
- 486 Bonan, G. B., P. J. Lawrence, K. W. Oleson, S. Levis, M. Jung, M. Reichstein,  
487 D. M. Lawrence, and S. C. Swenson (2011, may). Improving canopy pro-  
488 cesses in the Community Land Model version 4 (CLM4) using global flux  
489 fields empirically inferred from FLUXNET data. *Journal of Geophysical Re-*  
490 *search* 116(G2), G02014.
- 491 Booth, B. B. B., C. D. Jones, M. Collins, I. J. Totterdell, P. M. Cox, S. Sitch,  
492 C. Huntingford, R. A. Betts, G. R. Harris, and J. Lloyd (2012, jun). High  
493 sensitivity of future global warming to land carbon cycle processes. *Envi-*  
494 *ronmental Research Letters* 7(2), 024002.
- 495 Brix, H. (1971). Effects of nitrogen fertilization on photosynthesis and respira-  
496 tion in Douglas fir. *Forest Science* 17(4), 407–414.
- 497 Clark, D. B., L. M. Mercado, S. Sitch, C. D. Jones, N. Gedney, M. J. Best,  
498 M. Pryor, G. G. Rooney, R. L. H. Essery, E. Blyth, O. Boucher, R. J.  
499 Harding, C. Huntingford, and P. M. Cox (2011, sep). The Joint UK Land  
500 Environment Simulator (JULES), model description – Part 2: Carbon fluxes  
501 and vegetation dynamics. *Geoscientific Model Development* 4(3), 701–722.
- 502 Cornwell, W. K., J. H. C. Cornelissen, K. Amatangelo, E. Dorrepaal, V. T.



- 503 Eviner, O. Godoy, S. E. Hobbie, B. Hoorens, H. Kurokawa, N. Pérez-  
504 Harguindeguy, H. M. Quested, L. S. Santiago, D. A. Wardle, I. J. Wright,  
505 R. Aerts, S. D. Allison, P. van Bodegom, V. Brovkin, A. Chatain, T. V.  
506 Callaghan, S. Díaz, E. Garnier, D. E. Gurvich, E. Kazakou, J. A. Klein,  
507 J. Read, P. B. Reich, N. A. Soudzilovskaia, M. V. Vaieretti, and M. West-  
508 oby (2008, oct). Plant species traits are the predominant control on litter  
509 decomposition rates within biomes worldwide. *Ecology Letters* 11(10), 1065–  
510 1071.
- 511 Davies-Barnard, T., J. Meyerholt, S. Zaehle, P. Friedlingstein, V. Brovkin,  
512 Y. Fan, R. A. Fisher, C. D. Jones, H. Lee, D. Peano, B. Smith, D. Wårlind,  
513 and A. J. Wiltshire (2020, oct). Nitrogen cycling in CMIP6 land surface  
514 models: progress and limitations. *Biogeosciences* 17(20), 5129–5148.
- 515 Delaire, M., E. Frak, M. Sigogne, B. Adam, F. Beaujard, and X. Le Roux (2005,  
516 feb). Sudden increase in atmospheric CO<sub>2</sub> concentration reveals strong cou-  
517 pling between shoot carbon uptake and root nutrient uptake in young walnut  
518 trees. *Tree Physiology* 25(2), 229–235.
- 519 Dovrat, G., H. Bakhshian, T. Masci, and E. Sheffer (2020, jul). The nitro-  
520 gen economic spectrum of legume stoichiometry and fixation strategy. *New*  
521 *Phytologist* 227(2), 365–375.
- 522 Dovrat, G., T. Masci, H. Bakhshian, E. Mayzlish Gati, S. Golan, and E. Sheffer  
523 (2018, jul). Drought-adapted plants dramatically downregulate dinitrogen  
524 fixation: Evidences from Mediterranean legume shrubs. *Journal of Ecol-*  
525 *ogy* 106(4), 1534–1544.
- 526 Evans, J. R. and J. R. Seemann (1989). The allocation of protein nitrogen in

- 527 the photosynthetic apparatus: costs, consequences, and control. *Photosyn-*  
528 *thesis* 8, 183–205.
- 529 Exbrayat, J.-F., A. A. Bloom, P. Falloon, A. Ito, T. L. Smallman, and  
530 M. Williams (2018). Reliability ensemble averaging of 21st century pro-  
531 jections of terrestrial net primary productivity reduces global and regional  
532 uncertainties. *Earth System Dynamics* 9(1), 153–165.
- 533 Farquhar, G. D., S. von Caemmerer, and J. A. Berry (1980). A biochem-  
534 ical model of photosynthetic CO<sub>2</sub> assimilation in leaves of C<sub>3</sub> species.  
535 *Planta* 149(1), 78–90.
- 536 Firn, J., J. M. McGree, E. Harvey, H. Flores-Moreno, M. Schütz, Y. M. Buck-  
537 ley, E. T. Borer, E. W. Seabloom, K. J. La Pierre, A. M. MacDougall, S. M.  
538 Prober, C. J. Stevens, L. L. Sullivan, E. Porter, E. Ladouceur, C. Allen,  
539 K. H. Moromizato, J. W. Morgan, W. S. Harpole, Y. Hautier, N. Eisen-  
540 hauer, J. P. Wright, P. B. Adler, C. A. Arnillas, J. D. Bakker, L. Bieder-  
541 man, A. A. D. Broadbent, C. S. Brown, M. N. Bugalho, M. C. Caldeira,  
542 E. E. Cleland, A. Ebeling, P. A. Fay, N. Hagenah, A. R. Kleinhesselink,  
543 R. Mitchell, J. L. Moore, C. Nogueira, P. L. Peri, C. Roscher, M. D. Smith,  
544 P. D. Wragg, and A. C. Risch (2019, feb). Leaf nutrients, not specific leaf  
545 area, are consistent indicators of elevated nutrient inputs. *Nature Ecology*  
546 *Evolution* 3(3), 400–406.
- 547 Fisher, J. B., S. Sitch, Y. Malhi, R. A. Fisher, C. Huntingford, and S.-Y. Tan  
548 (2010). Carbon cost of plant nitrogen acquisition: A mechanistic, globally  
549 applicable model of plant nitrogen uptake, retranslocation, and fixation.  
550 *Global Biogeochemical Cycles* 24(1), 1–17.

- 551 Fox, J. and S. Weisberg (2019). *An R companion to applied regression* (Third  
552 edit ed.). Thousand Oaks, California: Sage.
- 553 Franklin, O., R. E. McMurtrie, C. M. Iversen, K. Y. Crous, A. C. Finzi, D. Tis-  
554 sue, D. S. Ellsworth, R. Oren, and R. J. Norby (2009, jan). Forest fine-root  
555 production and nitrogen use under elevated CO<sub>2</sub>: contrast-  
556 ing responses in evergreen and deciduous trees explained by a common prin-  
557 ciple. *Global Change Biology* 15(1), 132–144.
- 558 Friedlingstein, P., M. Meinshausen, V. K. Arora, C. D. Jones, A. Anav, S. K.  
559 Liddicoat, and R. Knutti (2014). Uncertainties in CMIP5 climate projections  
560 due to carbon cycle feedbacks. *Journal of Climate* 27(2), 511–526.
- 561 Friel, C. A. and M. L. Friesen (2019, nov). Legumes modulate allocation to  
562 rhizobial nitrogen fixation in response to factorial light and nitrogen manip-  
563 ulation. *Frontiers in Plant Science* 10, 1316.
- 564 Fujikake, H., A. Yamazaki, N. Ohtake, K. Sueoshi, S. Matsushashi, T. Ito,  
565 C. Mizuniwa, T. Kume, S. Hoshimoto, N.-S. Ishioka, S. Watanabe, A. Osa,  
566 T. Sekine, H. Uchida, A. Tsuji, and T. Ohyama (2003, may). Quick  
567 and reversible inhibition of soybean root nodule growth by nitrate in-  
568 volves a decrease in sucrose supply to nodules. *Journal of Experimental*  
569 *Botany* 54(386), 1379–1388.
- 570 Giardina, C. P., M. D. Coleman, J. E. Hancock, J. S. King, E. A. Lilleskov,  
571 W. M. Loya, K. S. Pregitzer, M. G. Ryan, and C. C. Trettin (2005). The  
572 response of belowground carbon allocation in forests to global change. In  
573 D. Binkley and O. Manyailo (Eds.), *Tree Species Effects on Soils: Implica-*  
574 *tions for Global Change* (Volume 55 ed.), Chapter Chapter 7, pp. 119–154.

- 575 Berlin/Heidelberg: Springer-Verlag.
- 576 Gibson, A. H. and J. E. Harper (1985, may). Nitrate effect on nodulation of  
 577 soybean by *Bradyrhizobium japonicum*. *Crop Science* 25(3), 497–  
 578 501.
- 579 Gill, A. L. and A. C. Finzi (2016). Belowground carbon flux links biogeochemical  
 580 cycles and resource-use efficiency at the global scale. *Ecology Letters* 19(12),  
 581 1419–1428.
- 582 Goll, D. S., V. Brovkin, B. R. Parida, C. H. Reick, J. Kattge, P. B. Reich,  
 583 P. M. van Bodegom, and Ü. Niinemets (2012, mar). Nutrient limitation  
 584 reduces land carbon uptake in simulations with a model of combined carbon,  
 585 nitrogen and phosphorus cycling. *Biogeosciences Discussions* 9(3), 3173–  
 586 3232.
- 587 Gulmon, S. L. and C. C. Chu (1981, may). The effects of light and nitrogen  
 588 on photosynthesis, leaf characteristics, and dry matter allocation in the  
 589 chaparral shrub, *Diplacus aurantiacus*. *Oecologia* 49(2), 207–212.
- 590 Gutschick, V. P. (1981, nov). Evolved strategies in nitrogen acquisition by  
 591 plants. *The American Naturalist* 118(5), 607–637.
- 592 Henneron, L., P. Kardol, D. A. Wardle, C. Cros, and S. Fontaine (2020, nov).  
 593 Rhizosphere control of soil nitrogen cycling: a key component of plant eco-  
 594 nomic strategies. *New Phytologist* 228(4), 1269–1282.
- 595 Hoagland, D. R. and D. I. Arnon (1950). The water-culture method for growing  
 596 plants without soil. *California Agricultural Experiment Station: 347* 347(2),  
 597 1–32.

- 598 Hobbie, E. A. (2006, mar). Carbon allocation to ectomycorrhizal fungi corre-  
 599 lates with belowground allocation in culture studies. *Ecology* 87(3), 563–569.
- 600 Hobbie, E. A. and J. E. Hobbie (2008, aug). Natural abundance of  $^{15}\text{N}$  in  
 601 nitrogen-limited forests and tundra can estimate nitrogen cycling through  
 602 mycorrhizal fungi: a review. *Ecosystems* 11(5), 815–830.
- 603 Hoek, T. A., K. Axelrod, T. Biancalani, E. A. Yurtsev, J. Liu, and J. Gore  
 604 (2016, aug). Resource availability modulates the cooperative and compet-  
 605 itive nature of a microbial cross-feeding mutualism. *PLOS Biology* 14(8),  
 606 e1002540.
- 607 Högborg, M. N., M. J. I. Briones, S. G. Keel, D. B. Metcalfe, C. Campbell,  
 608 A. J. Midwood, B. Thornton, V. Hurry, S. Linder, T. Näsholm, and P. Hög-  
 609 berg (2010, jul). Quantification of effects of season and nitrogen supply on  
 610 tree below-ground carbon transfer to ectomycorrhizal fungi and other soil  
 611 organisms in a boreal pine forest. *New Phytologist* 187(2), 485–493.
- 612 Högborg, P., M. N. Högborg, S. G. Göttlicher, N. R. Betson, S. G. Keel, D. B.  
 613 Metcalfe, C. Campbell, A. Schindlbacher, V. Hurry, T. Lundmark, S. Lin-  
 614 der, and T. Näsholm (2008, jan). High temporal resolution tracing of pho-  
 615 tosynthate carbon from the tree canopy to forest soil microorganisms. *New*  
 616 *Phytologist* 177(1), 220–228.
- 617 Houlton, B. Z., Y.-P. Wang, P. M. Vitousek, and C. B. Field (2008, jul). A  
 618 unifying framework for dinitrogen fixation in the terrestrial biosphere. *Na-*  
 619 *ture* 454(7202), 327–330.
- 620 Johnson, N. C., J. H. Graham, and F. A. Smith (1997, apr). Functioning of  
 621 mycorrhizal associations along the mutualism-parasitism continuum. *New*

- 622**      *Phytologist* 135(4), 575–585.
- 623**      Kaiser, C., M. R. Kilburn, P. L. Clode, L. Fuchslueger, M. Koranda, J. B. Cliff,  
**624**      Z. M. Solaiman, and D. V. Murphy (2015, mar). Exploring the transfer of  
**625**      recent plant photosynthates to soil microbes: mycorrhizal pathway vs direct  
**626**      root exudation. *New Phytologist* 205(4), 1537–1551.
- 627**      Kattge, J., W. Knorr, T. Raddatz, and C. Wirth (2009). Quantifying photosyn-  
**628**      thetic capacity and its relationship to leaf nitrogen content for global-scale  
**629**      terrestrial biosphere models. *Global Change Biology* 15(4), 976–991.
- 630**      Kayler, Z., A. Gessler, and N. Buchmann (2010, sep). What is the speed of link  
**631**      between aboveground and belowground processes? *New Phytologist* 187(4),  
**632**      885–888.
- 633**      Kayler, Z., C. Keitel, K. Jansen, and A. Gessler (2017, mar). Experimental  
**634**      evidence of two mechanisms coupling leaf-level C assimilation to rhizosphere  
**635**      CO<sub>2</sub> release. *Environmental and Experimental Botany* 135,  
**636**      21–26.
- 637**      Kenward, M. G. and J. H. Roger (1997, sep). Small sample inference for fixed  
**638**      effects from restricted maximum likelihood. *Biometrics* 53(3), 983.
- 639**      Knorr, W. (2000, jun). Annual and interannual CO<sub>2</sub> exchanges  
**640**      of the terrestrial biosphere: process-based simulations and uncertainties.  
**641**      *Global Ecology and Biogeography* 9(3), 225–252.
- 642**      Knorr, W. and M. Heimann (2001, mar). Uncertainties in global terrestrial bio-  
**643**      sphere modeling: 1. A comprehensive sensitivity analysis with a new photo-  
**644**      synthesis and energy balance scheme. *Global Biogeochemical Cycles* 15(1),

- 645 207–225.
- 646 Kulmatiski, A., P. B. Adler, J. M. Stark, and A. T. Tredennick (2017, mar).  
647 Water and nitrogen uptake are better associated with resource availability  
648 than root biomass. *Ecosphere* 8(3), e01738.
- 649 Lawrence, D. M., R. A. Fisher, C. D. Koven, K. W. Oleson, S. C. Swen-  
650 son, G. B. Bonan, N. Collier, B. Ghimire, L. Kampenhout, D. Kennedy,  
651 E. Kluzek, P. J. Lawrence, F. Li, H. Li, D. L. Lombardozzi, W. J. Riley,  
652 W. J. Sacks, M. Shi, M. Vertenstein, W. R. Wieder, C. Xu, A. A. Ali,  
653 A. M. Badger, G. Bisht, M. Broeke, M. A. Brunke, S. P. Burns, J. Buzan,  
654 M. Clark, A. Craig, K. M. Dahlin, B. Drewniak, J. B. Fisher, M. Flan-  
655 ner, A. M. Fox, P. Gentine, F. M. Hoffman, G. Keppel-Aleks, R. Knox,  
656 S. Kumar, J. Lenaerts, L. R. Leung, W. H. Lipscomb, Y. Lu, A. Pandey,  
657 J. D. Pelletier, J. Perket, J. T. Randerson, D. M. Ricciuto, B. M. Sander-  
658 son, A. Slater, Z. M. Subin, J. Tang, R. Q. Thomas, M. Val Martin, and  
659 X. Zeng (2019, dec). The Community Land Model Version 5: description of  
660 new features, benchmarking, and impact of forcing uncertainty. *Journal of*  
661 *Advances in Modeling Earth Systems* 11(12), 4245–4287.
- 662 LeBauer, D. S. and K. Treseder (2008). Nitrogen limitation of net primary  
663 productivity. *Ecology* 89(2), 371–379.
- 664 Lenth, R. (2019). emmeans: estimated marginal means, aka least-squares  
665 means.
- 666 Li, W., H. Zhang, G. Huang, R. Liu, H. Wu, C. Zhao, and N. G. McDowell  
667 (2020, mar). Effects of nitrogen enrichment on tree carbon allocation: A  
668 global synthesis. *Global Ecology and Biogeography* 29(3), 573–589.

- 669 Liang, J., X. Qi, L. Souza, and Y. Luo (2016, may). Processes regulating pro-  
670 gressive nitrogen limitation under elevated carbon dioxide: a meta-analysis.  
671 *Biogeosciences* 13(9), 2689–2699.
- 672 Liang, X., T. Zhang, X. Lu, D. S. Ellsworth, H. BassiriRad, C. You, D. Wang,  
673 P. He, Q. Deng, H. Liu, J. Mo, and Q. Ye (2020, jun). Global response pat-  
674 terns of plant photosynthesis to nitrogen addition: A meta-analysis. *Global*  
675 *Change Biology* 26(6), 3585–3600.
- 676 Luo, Y., W. S. Currie, J. S. Dukes, A. C. Finzi, U. A. Hartwig, B. A. Hungate,  
677 R. E. McMurtrie, R. Oren, W. J. Parton, D. E. Pataki, R. M. Shaw, D. R.  
678 Zak, and C. B. Field (2004). Progressive nitrogen limitation of ecosystem  
679 responses to rising atmospheric carbon dioxide. *BioScience* 54(8), 731–739.
- 680 Markham, J. H. and C. Zekveld (2007, sep). Nitrogen fixation makes biomass  
681 allocation to roots independent of soil nitrogen supply. *Canadian Journal*  
682 *of Botany* 85(9), 787–793.
- 683 Masson-Delmotte, V., P. Zhai, A. Pirani, S. L. Connors, S. Berger, N. Caud,  
684 Y. Chen, L. Goldfarb, M. I. Gomis, M. Huang, K. Leitzell, E. Lonnoy,  
685 J. B. R. Matthews, T. K. Maycock, T. Waterfield, O. Yelekçi, R. Yu, and  
686 B. Zhou (2021). *Climate Change 2021: The Physical Science Basis. Contri-*  
687 *bution of Working Group I to the Sixth Assessment Report of the Intergov-*  
688 *ernmental Panel on Climate Change*. Cambridge, UK and New York, USA:  
689 Cambridge University Press.
- 690 Matamala, R. and W. H. Schlesinger (2000, dec). Effects of elevated atmo-  
691 spheric CO<sub>2</sub> on fine root production and activity in an intact  
692 temperate forest ecosystem. *Global Change Biology* 6(8), 967–979.



- 693 Menge, D. N. L., S. A. Levin, and L. O. Hedin (2008, feb). Evolutionary trade-  
 694 offs can select against nitrogen fixation and thereby maintain nitrogen limi-  
 695 tation. *Proceedings of the National Academy of Sciences* 105(5), 1573–1578.
- 696 Meyerholt, J., S. Zaehle, and M. J. Smith (2016, mar). Variability of pro-  
 697 jected terrestrial biosphere responses to elevated levels of atmospheric  
 698 CO<sub>2</sub> due to uncertainty in biological nitrogen fixation. *Bio-*  
 699 *geosciences* 13(5), 1491–1518.
- 700 Muñoz, N., X. Qi, M. W. Li, M. Xie, Y. Gao, M. Y. Cheung, F. L. Wong, and  
 701 H.-M. Lam (2016). Improvement in nitrogen fixation capacity could be part  
 702 of the domestication process in soybean. *Heredity* 117(2), 84–93.
- 703 Nadelhoffer, K. J. and J. W. Raich (1992, aug). Fine root production estimates  
 704 and belowground carbon allocation in forest ecosystems. *Ecology* 73(4),  
 705 1139–1147.
- 706 Norby, R. J., J. Ledford, C. D. Reilly, N. E. Miller, and E. G. O’Neill (2004,  
 707 jun). Fine-root production dominates response of a deciduous forest to at-  
 708 mospheric CO<sub>2</sub> enrichment. *Proceedings of the National Academy of Sci-*  
 709 *ences* 101(26), 9689–9693.
- 710 Noyce, G. L., M. L. Kirwan, R. L. Rich, and J. P. Megonigal (2019). Asyn-  
 711 chronous nitrogen supply and demand produce nonlinear plant allocation  
 712 responses to warming and elevated CO<sub>2</sub>. *Proceedings of the*  
 713 *National Academy of Sciences* 116(43), 21623–21628.
- 714 Parvin, S., S. Uddin, S. Tausz-Posch, R. Armstrong, and M. Tausz (2020,  
 715 jul). Carbon sink strength of nodules but not other organs modulates  
 716 photosynthesis of faba bean (*Vicia faba*) grown under elevated

- 717 [CO<sub>2</sub>] and different water supply. *New Phytologist* 227(1),  
718 132–145.
- 719 Phillips, R. P., E. R. Brzostek, and M. G. Midgley (2013). The mycorrhizal-  
720 associated nutrient economy: a new framework for predicting carbon-  
721 nutrient couplings in temperate forests. *New Phytologist* 199(1), 41–51.
- 722 Phillips, R. P., A. C. Finzi, and E. S. Bernhardt (2011, feb). Enhanced root  
723 exudation induces microbial feedbacks to N cycling in a pine forest under  
724 long-term CO<sub>2</sub> fumigation. *Ecology Letters* 14(2), 187–194.
- 725 Poorter, H., J. Bühler, D. Van Dusschoten, J. Climent, and J. A. Postma (2012).  
726 Pot size matters: A meta-analysis of the effects of rooting volume on plant  
727 growth. *Functional Plant Biology* 39(11), 839–850.
- 728 Prentice, I. C., X. Liang, B. E. Medlyn, and Y.-P. Wang (2015). Reliable, ro-  
729 bust and realistic: The three R’s of next-generation land-surface modelling.  
730 *Atmospheric Chemistry and Physics* 15, 5987–6005.
- 731 R Core Team (2021). R: A language and environment for statistical computing.
- 732 Raich, J. W., D. A. Clark, L. Schwendenmann, and T. E. Wood (2014, jun).  
733 Aboveground tree growth varies with belowground carbon allocation in a  
734 tropical rainforest environment. *PLoS ONE* 9(6), e100275.
- 735 Rastetter, E. B., P. M. Vitousek, C. B. Field, G. R. Shaver, D. Herbert, and G. I.  
736 Ågren (2001, jul). Resource optimization and symbiotic nitrogen fixation.  
737 *Ecosystems* 4(4), 369–388.
- 738 Rogers, A. (2014, feb). The use and misuse of V<sub>c,max</sub> in Earth  
739 System Models. *Photosynthesis Research* 119(1-2), 15–29.

- 740 Rogers, A., B. E. Medlyn, J. S. Dukes, G. B. Bonan, S. Caemmerer, M. C.  
741 Dietze, J. Kattge, A. D. B. Leakey, L. M. Mercado, Ü. Niinemets, I. C.  
742 Prentice, S. P. Serbin, S. Sitch, D. A. Way, and S. Zaehle (2017, jan). A  
743 roadmap for improving the representation of photosynthesis in Earth system  
744 models. *New Phytologist* 213(1), 22–42.
- 745 Saleh, A. M., M. Abdel-Mawgoud, A. R. Hassan, T. H. Habeeb, R. S. Yehia, and  
746 H. AbdElgawad (2020, jun). Global metabolic changes induced by arbuscu-  
747 lar mycorrhizal fungi in oregano plants grown under ambient and elevated  
748 levels of atmospheric CO<sub>2</sub>. *Plant Physiology and Biochem-*  
749 *istry* 151, 255–263.
- 750 Schaefer, K., C. R. Schwalm, C. Williams, M. A. Arain, A. Barr, J. M. Chen,  
751 K. J. Davis, D. Dimitrov, T. W. Hilton, D. Y. Hollinger, E. Humphreys,  
752 B. Poulter, B. M. Raczka, A. D. Richardson, A. Sahoo, P. Thornton, R. Var-  
753 gas, H. Verbeeck, R. Anderson, I. Baker, T. A. Black, P. Bolstad, J. Chen,  
754 P. S. Curtis, A. R. Desai, M. C. Dietze, D. Dragoni, C. M. Gough, R. F.  
755 Grant, L. Gu, A. K. Jain, C. Kucharik, B. E. Law, S. Liu, E. Lokipitiya,  
756 H. A. Margolis, R. Matamala, J. H. McCaughey, R. Monson, J. W. Munger,  
757 W. Oechel, C. Peng, D. T. Price, D. Ricciuto, W. J. Riley, N. Roulet,  
758 H. Tian, C. Tonitto, M. Torn, E. Weng, and X. Zhou (2012, sep). A model-  
759 data comparison of gross primary productivity: Results from the North  
760 American Carbon Program site synthesis. *Journal of Geophysical Research:*  
761 *Biogeosciences* 117(G3), G03010.
- 762 Shi, M., J. B. Fisher, E. R. Brzostek, and R. P. Phillips (2016). Carbon cost  
763 of plant nitrogen acquisition: Global carbon cycle impact from an improved

- 764 plant nitrogen cycle in the Community Land Model. *Global Change Biol-*  
765 *ogy* 22(3), 1299–1314.
- 766 Shi, M., J. B. Fisher, R. P. Phillips, and E. R. Brzostek (2019, jan). Neglect-  
767 ing plant–microbe symbioses leads to underestimation of modeled climate  
768 impacts. *Biogeosciences* 16(2), 457–465.
- 769 Smith, N. G. and J. S. Dukes (2013, jan). Plant respiration and photosynthesis  
770 in global-scale models: incorporating acclimation to temperature and CO  
771 2. *Global Change Biology* 19(1), 45–63.
- 772 Smith, N. G., D. L. Lombardozzi, A. Tawfik, G. B. Bonan, and J. S. Dukes  
773 (2017, mar). Biophysical consequences of photosynthetic temperature accli-  
774 mation for climate. *Journal of Advances in Modeling Earth Systems* 9(1),  
775 536–547.
- 776 Smith, N. G., S. L. Malyshev, E. Shevliakova, J. Kattge, and J. S. Dukes (2016,  
777 apr). Foliar temperature acclimation reduces simulated carbon sensitivity  
778 to climate. *Nature Climate Change* 6(4), 407–411.
- 779 Soudzilovskaia, N. A., J. C. Douma, A. A. Akhmetzhanova, P. M. van Bode-  
780 gom, W. K. Cornwell, E. J. Moens, K. K. Treseder, and J. H. C. Cornelissen  
781 (2015). Global patterns of plant root colonization intensity by mycorrhizal  
782 fungi explained by climate and soil chemistry. *Global Ecology and Biogeog-*  
783 *raphy* 24(3), 371–382.
- 784 Sulman, B. N., E. Shevliakova, E. R. Brzostek, S. N. Kivlin, S. L. Malyshev,  
785 D. N. L. Menge, and X. Zhang (2019). Diverse mycorrhizal associations  
786 enhance terrestrial C storage in a global model. *Global Biogeochemical Cy-*  
787 *cles* 33(4), 501–523.

- 788 Taylor, B. N. and D. N. L. Menge (2018, sep). Light regulates tropical symbiotic  
789 nitrogen fixation more strongly than soil nitrogen. *Nature Plants* 4(9), 655–  
790 661.
- 791 Terrer, C., S. Vicca, B. D. Stocker, B. A. Hungate, R. P. Phillips, P. B. Reich,  
792 A. C. Finzi, and I. C. Prentice (2018, jan). Ecosystem responses to elevated  
793  $\text{CO}_2$  governed by plant–soil interactions and  
794 the cost of nitrogen acquisition. *New Phytologist* 217(2), 507–522.
- 795 Thomas, R. Q., E. N. J. Brookshire, and S. Gerber (2015, may). Nitrogen  
796 limitation on land: how can it occur in Earth system models? *Global Change*  
797 *Biology* 21(5), 1777–1793.
- 798 Thomas, R. Q., S. Zaehle, P. H. Templer, and C. L. Goodale (2013, oct). Global  
799 patterns of nitrogen limitation: confronting two global biogeochemical mod-  
800 els with observations. *Global Change Biology* 19(10), 2986–2998.
- 801 Thornton, P. E., J.-F. Lamarque, N. A. Rosenbloom, and N. M. Mahowald  
802 (2007, dec). Influence of carbon-nitrogen cycle coupling on land model re-  
803 sponse to  $\text{CO}_2$  fertilization and climate variability. *Global*  
804 *Biogeochemical Cycles* 21(4), GB4018.
- 805 Tingey, D. T., D. L. Phillips, and M. G. Johnson (2000, jul). Elevated  
806  $\text{CO}_2$  and conifer roots: effects on growth, life span and  
807 turnover. *New Phytologist* 147(1), 87–103.
- 808 Uselman, S. M., R. G. Qualls, and R. B. Thomas (2000). Effects of increased  
809 atmospheric  $\text{CO}_2$ , temperature, and soil N availability on  
810 root exudation of dissolved organic carbon by a N-fixing tree (*Robinia*  
811 *pseudoacacia* L.). *Plant and Soil* 222, 191–202.

- 812 van Diepen, L. T. A., E. A. Lilleskov, K. S. Pregitzer, and R. M. Miller (2007,  
813 oct). Decline of arbuscular mycorrhizal fungi in northern hardwood forests  
814 exposed to chronic nitrogen additions. *New Phytologist* 176(1), 175–183.
- 815 Vitousek, P. M., K. Cassman, C. C. Cleveland, T. Crews, C. B. Field, N. B.  
816 Grimm, R. W. Howarth, R. Marino, L. Martinelli, E. B. Rastetter, and  
817 J. I. Sprent (2002). Towards an ecological understanding of biological nitro-  
818 gen fixation. In *The Nitrogen Cycle at Regional to Global Scales*, pp. 1–45.  
819 Dordrecht: Springer Netherlands.
- 820 Vitousek, P. M. and R. W. Howarth (1991). Nitrogen limitation on land and in  
821 sea: how can it occur? *Biogeochemistry* 13(2), 87–115.
- 822 Vitousek, P. M., S. Porder, B. Z. Houlton, and O. A. Chadwick (2010, jan).  
823 Terrestrial phosphorus limitation: mechanisms, implications, and nitro-  
824 gen–phosphorus interactions. *Ecological Applications* 20(1), 5–15.
- 825 Walker, A. P., A. P. Beckerman, L. Gu, J. Kattge, L. A. Cernusak, T. F.  
826 Domingues, J. C. Scales, G. Wohlfahrt, S. D. Wullschleger, and F. I. Wood-  
827 ward (2014, aug). The relationship of leaf photosynthetic traits - V<sub>max</sub>  
828 and J<sub>max</sub> - to leaf nitrogen, leaf phosphorus, and specific leaf area: a meta-  
829 analysis and modeling study. *Ecology and Evolution* 4(16), 3218–3235.
- 830 Wang, W., Y. Wang, G. Hoch, Z. Wang, and J. Gu (2018, apr). Linkage of  
831 root morphology to anatomy with increasing nitrogen availability in six  
832 temperate tree species. *Plant and Soil* 425(1-2), 189–200.
- 833 Wieder, W. R., C. C. Cleveland, W. K. Smith, and K. Todd-Brown (2015).  
834 Future productivity and carbon storage limited by terrestrial nutrient avail-  
835 ability. *Nature Geoscience* 8(6), 441–444.

- 836 Wieder, W. R., D. M. Lawrence, R. A. Fisher, G. B. Bonan, S. J. Cheng, C. L.  
 837 Goodale, A. S. Grandy, C. D. Koven, D. L. Lombardozzi, K. W. Oleson, and  
 838 R. Q. Thomas (2019, oct). Beyond static benchmarking: using experimental  
 839 manipulations to evaluate land model assumptions. *Global Biogeochemical*  
 840 *Cycles* 33(10), 1289–1309.
- 841 Xu-Ri and I. C. Prentice (2017, apr). Modelling the demand for new nitrogen  
 842 fixation by terrestrial ecosystems. *Biogeosciences* 14(7), 2003–2017.
- 843 Zaehle, S., S. Sitch, B. Smith, and F. Hatterman (2005, sep). Effects of param-  
 844 eter uncertainties on the modeling of terrestrial biosphere dynamics. *Global*  
 845 *Biogeochemical Cycles* 19(3), GB3020.
- 846 Zhu, Q., W. J. Riley, J. Tang, N. Collier, F. M. Hoffman, X. Yang, and G. Bisht  
 847 (2019). Representing nitrogen, phosphorus, and carbon interactions in the  
 848 E3SM land model: development and global benchmarking. *Journal of Ad-*  
 849 *vances in Modeling Earth Systems* 11(7), 2238–2258.
- 850 Ziehn, T., J. Kattge, W. Knorr, and M. Scholze (2011, may). Improving the  
 851 predictability of global CO<sub>2</sub> assimilation rates under climate change. *Geo-*  
 852 *physical Research Letters* 38(10), L10404.